 doi:10.20944/preprints202202.0223.v1

Article

Dolutegravir Inhibits Proliferation and Motility of BT-20 Tumor Cells through Inhibition of Human Endogenous Retrovirus Type K

Jiayi Li[1], John Lin[1], John R. Lin[1], Mason Farris[1], Lauren Robbins[1], Leo Andrada[1], Bryce Grohol[1], Serratt Nong[1] and Yingguang Liu[1,*]

[1] College of Osteopathic Medicine, Liberty University, 306 Liberty View Lane, Lynchburg, Virginia 24502, United States of America; jli16@liberty.edu; jlin1@liberty.edu; jlin@liberty.edu; mfarris3@liberty.edu; ldrobbins@liberty.edu; landrada@liberty.edu; bgrohol@liberty.edu; srnong@liberty.edu

* Correspondence: yliu@liberty.edu; Tel., 001-434-592-7344

Abstract: Increasing evidence points to the role of endogenous retroviruses (ERVs) in driving cancer cell proliferation. The purpose of this study was to explore the possibility of repurposing antiretroviral agents to inhibit ERVs as a new approach in cancer treatment. We found that an integrase strand-transfer inhibitor, dolutegravir (DTG), effectively inhibited the proliferation of multiple cancer cell lines and its antiproliferative potency was positively correlated with the expression levels of the human endogenous retrovirus type K (HERV-K). DTG inhibited the expression of HERV-K in multiple human cancer cell lines and the mouse mammary tumor virus (MMTV) in the murine 4T1 mammary cancer cell line. We chose the fast-growing BT-20 cell line as a model to study the *in vitro* antiproliferative mechanisms of DTG. BT-20 cells overexpressing both HERV-K *env* and *pol* genes became more resistant to DTG than cells transduced with vector alone. Knockdown of HERV-K also increased DTG resistance of BT-20 cells. The antiproliferative effect of DTG correlated with enhanced expression of E-cadherin and reduction in cell motility and invasiveness. Surprisingly, DTG stimulated expression of the *env* gene of MMTV *in vivo* and promoted metastasis of 4T1 tumor cells to the lungs. Taken together, our data support a role of ERVs in tumor development and encourage further search for antiretroviral agents to treat malignancies in which endogenous retroviruses are active.

Keywords: endogenous retroviruses; HERV-K; mouse mammary tumor virus; dolutegravir; 4T1 cells; metastasis

1. Introduction

Endogenous retroviruses (ERVs) are repetitive DNA sequences in eukaryotic genomes that resemble DNA genomes of retroviruses. ERVs constitute significant portions of mammalian genomes. Instead of being acquired through infection of exogenous viruses, ERVs are transmitted vertically in the Mendelian fashion. Most human ERVs are degenerate and cannot produce infectious viral particles for horizontal transmission. ERVs may play important roles in embryonic development [1], and like other genes essential for early development, ERV genes are actively expressed in many malignancies [2]. Moreover, the Env protein of one group of human ERV, HERV-K, has been demonstrated to induce cell proliferation, migration, invasion, tumor formation, and epithelial to mesenchymal transition through the ERK1/2 pathway [3,4]. In addition, the long terminal repeat of HERV-K is integrated into progesterone-driven breast cancer cell proliferation [5]. Consequently, there have been explorations to target ERVs as an approach in cancer therapy [6,7]. Antiretroviral agents used to treat HIV/AIDS including reverse transcriptase inhibitors (RTI), protease inhibitors (PI), and integrase strand-transfer inhibitors (INSTI), have been found effective in inhibiting HERV-K replication [8]. Some antiretroviral drugs have been shown to be effective in suppressing tumor cell growth *in vitro* and *in vivo*

 doi:10.20944/preprints202202.0223.v1

[**Error! Bookmark not defined.**,**Error! Bookmark not defined.**,9,10]. However, the antineoplastic effect of these agents has not been attributed to their antiviral effects. For example, efavirenz, a non-nucleoside reverse transcriptase inhibitor, is found to target the reverse transcriptase of L1 elements, which is thought to be the chief antineoplastic mechanism [11]. Nelfinavir, a protease inhibitor, has been found to exert its antineoplastic effect through generation of reactive oxygen species (ROS) [12].

RTIs are not good tools to investigate the relationship between the antiretroviral effect and the antineoplastic effect because long interspersed nuclear elements (LINEs) also carry reverse transcriptase whose activation is a hallmark of cancer. On the other hand, PIs and INSTIs are more specific inhibitors of ERVs. Raltegravir (INSTI), darunavir (PI), and lopinavir (PI) have all been found to inhibit HERV-K [**Error! Bookmark not defined.**]. In the study reported below, we found that dolutegravir (DTG), an INSTI, has potent antiproliferative effects in cancer cells where HERV-K is active. Using overexpression and knockdown cell lines, we demonstrated that DTG exerts antiproliferative and anti-migration effects through inhibition of HERV-K, although the antiretroviral effect is not the only cytotoxic mechanism. We also tested the potential effect of DTG on tumor growth and metastasis in a mouse mammary cancer model where the mouse mammary tumor virus (MMTV, a homolog of HERV-K) is involved.

2. Materials and Methods

2.1. Cell Lines, Culture, and in Vitro Drug Treatment

BT-20 breast tumor cell line (kindly provided by Dr. Jiayuh Lin of the University of Maryland) was maintained in Eagle's Minimum Essential Medium (EMEM) with 10% fetal bovine serum (FBS) and 5% CO_2. T47D breast cancer cell line (kindly provided by Dr. Joseph Brewer of Via College of Osteopathic Medicine) and 4T1 murine mammary cancer cell line (American type culture collection, ATCC) were maintained in RPMI 1640 with 10% FBS and 5% CO_2. MBA-MD-453 breast cancer cell line (Lin) was maintained in Leibovitz's L-15 Medium in atmospheric air. SKBR3 breast cancer cell line (Lin), LNCaP prostate cancer cell line (ATCC), and HEK293T cells (ATCC) were maintained in Dulbecco's Modified Eagle Medium (DMEM) with 10% FBS and 5% CO_2. All cells were cultured at 37°C. Dolutegravir (DTG, Advanced ChemBlocks) was dissolved in dimethylsulfoxide (DMSO) and added to culture media at various concentrations. Cells were treated for 3-5 days in the presence of the drug, depending on cell line. For induction of ERV genes in overexpression cell lines, doxycycline (Cayman Chemical) was dissolved in DMSO and added to culture media at a final concentration of 0.1 mg/ml. The DMSO solvent was added to control cells. After incubation, cells were trypsinized and counted using a NucleoCounter-3000 (Chemometec) according to the manufacturer's instructions. Most counting was done with the Viability and Cell Count Assay, except for T47D cells which were counted with the Aggregated Cell Count Assay.

2.2. Extraction of RNA, Reverse Transcription and Quantitative PCR

Total cell RNA was extracted from cultured cells or homogenized tissues using the RNeasy Plus Mini Kit (Qiagen). Complementary DNA was prepared using the Quantitect Reverse Transcription Kit (Qiagen). Real-time PCR was performed using the LightCycler 96 (Roche) and SsoAdvanced Universal SYBR Green Supermix (Bio-Rad) or AzuraQuant Green Fast qPCR Mix (RealTimePrimers). A pair of primers targets the *pol* gene of HERV-K107 and HERV-K108 (See Table S1 for qPCR primers). Another pair of primers targets the *env* gene of HERV-K108. The *YWHAZ* gene encoding the 14-3-3 protein zeta/delta was used as the reference gene (for primer sequences, see [13]) for quantification of HERV-K transcripts. The *GAPDH* gene was used as a control for quantification of genomic HERV-K copies. For quantification of MMTV transcripts, the mouse gene for phosphoglycerate kinase 1 (Pgk1) was used as the reference. Primers of *Pgk1*, *YWHAZ*, and *GAPDH* were used at 100 nM. Primers for HERV-K and MMTV genes were used at 400 nM. HERV-K

Preprints (www.preprints.org) | NOT PEER-REVIEWED | Posted: 18 February 2022 doi:10.20944/preprints202202.0223.v1

genes and the human *YWHAZ* gene were amplified at 95°C 15″, 57°C 25″, 72°C 45″, while MMTV genes and the mouse Pgk1 gene were amplified at 95°C 15″, 58°C 25″, 72°C 45″.

For quantitation of HERV-K copies in genomic DNA, the Quick-DNA Miniprep Kit (Zymo Research) was used to extract the DNA. Primers for *env* and *pol* were the same as in the reverse-transcription PCR described above. The reference gene was also *YWHAZ*.

2.3. Plasmids and Constructs

The *env* and *pol* genes of HERV-K were amplified from BAC clones RP11-33P21 (containing the HERV-K108 sequence) and CTB-69E10 (containing the HERV-K107 gag-pro-pol gene) (See table S2 for primer sequences). The BAC clones were purchased from ThermoFisher. The *env* and *pol* genes of MMTV were amplified from mouse genomic DNA extracted from the 4T1 cell line. CloneAmp HiFi PCR Premix (Takarabio) was used to amplify the target genes. The lentiviral vector, pLenti-puro (Addgene), was digested with BstBI and BamHI for cloning of HERV-K genes. It was digested with EcoRI and XhoI for cloning MMTV *env* and with SpeI and MluI for cloning MMTV *pol*. In-Fusion® HD Cloning Plus Kit or In-Fusion Snap Assembly Master Mix (Takarabio) were used in making the overexpression constructs. For HERV-K knockdown, the ERVK-6 Human shRNA Plasmid Kit was purchased from OriGene (ERVK-6 is an alias for HERV-K108).

2.4. Lentiviral Packaging and Transduction

Overexpression constructs or shRNA knockdown plasmids were used to transfect HEK293 cells along with the packaging plasmid pCMV-dR8.2 dvpr (Addgene) and the *env*-expressing pCMV-VSV-G (Addgene) in an equimolar ratio. The Lipofectamine 3000 reagent and OptiMEM I reduced serum medium (both from ThermoFisher) were used in the transfection protocols according to manufacturer's instructions. Culture supernatant was used to transduce target cells in the presence of polybrene at 8 μg/m. For selection of transduced cells, puromycin concentration was gradually increased from 0.5 μg/mL to 1 μg/mL for both BT-20 and T47D cell lines.

2.5. Immunoblotting

Cells were lysed with RIPA buffer containing mammalian protease inhibitor cocktail (Genesee Scientific) and electrophorized in SDS-polyacrylamide gels. Samples were transferred electrically onto a nitrocellulose membrane. Polyclonal anti-ERK-9 Env (MyBioSource) and monoclonal anti-HERVK capsid (Austral Biological) were used at 1:5000. Monoclonal anti-E-Cadherin (American Research Products) was used at 1:20. Reaction with the above three primary antibodies were carried out at 4°C overnight. Monoclonal anti-V5 Tag (ThermoFisher) was used at 1:5,000 and incubated at room temperature for 1.5 hours. HRP-conjugated monoclonal anti-GAPDH (MyBioSource) was used at 1:40,000 and incubated at room temperature for 1 hour. HRP-conjugated goat anti-mouse IgG and HRP-conjugated goat anti-rabbit IgG (both from Bosterbio) were used at 1:20,000. Reaction with the above two secondary antibodies were carried out at room temperature for 1-1.5 hours. Enhanced chemiluminescence (Bosterbio) was photographed using the ChemiDoc XRS+ System (Bio-Rad).

2.6. Reactive Oxygen Species Assay

Intracellular ROS was quantified using the DCFDA/H2DCFDA-Cellular ROS Assay Kit (abcam) according to manufacturer's instructions. T47D cells were cultured in RPMI1640 medium without phenol red and seeded onto a clear-bottom 96-well microplate at 25,000 cells per well. Final concentration of dolutegravir was 20 μM and final concentration of nelfinavir (Sigma-Aldrich) was 10 μM. Samples were in triplicates. Fluorescence was read at Ex/Em = 485/520 nm in end point mode using the FLUOstar® Omega microplate reader (BMG).

2.7. Cell Cycle Analysis

Preprints (www.preprints.org) | NOT PEER-REVIEWED | Posted: 18 February 2022 doi:10.20944/preprints202202.0223.v1

The NucleoCounter-3000 (Chemometec) was used to perform the DAPI-based 2-Step Cell Cycle Assay according to manufacturer's instructions.

2.8. Wound Healing Assay

BT-20 cells were pre-treated with 50-μM DTG or DMSO for 48 hours and seeded in quadruplet wells on a 24-well plate in serum-free EMEM. DTG-treated cells continued to receive the same concentration of drug during wound healing. After allowing 4 hours for attachment, cells were scratched and photographed at 4x for 22 hours at 30-minute intervals using a BZ-X800 microscope (Keyence) while the cells are incubated at 37°C with 5% CO_2. Relative wound density was calculated according to [14].

2.9. Transwell Invasion Assay

Transwell Invasion Assay was performed using the Cultrex Basement Membrane Extract Cell Invasion Assay Kit (R&D Systems). Top wells were treated with 0.1x or 0.5x basement membrane extract. BT-20 cells were pretreated with 50-μM DTG or DMSO solvent for 24 hours and seeded in top wells of a 96-well plate at $3x10^4$ cells per well in DMEM with 0.5% FBS. DTG-treated cells were continuously treated with the same concentration of drug during the assay. After incubation for 65 hours, cells in top wells were trypsinized and counted using the NucleoCounter-3000, while cells in the bottom wells were stained with crystal violet and counted using the Image Cytometry function of the BZ-X800 microscope (Keyence).

2.10. Inoculation and Treatment of Mice

BALB/c mice 7-8 weeks old were inoculated with 15,000 4T1 cells suspended in 50 μL of Versene solution (ThermoFisher) subcutaneously using a 30½-gage needle into the 4th mammary gland. Treatment with DTG was administered on the same day and every day for 32 days. The drug was suspended in phosphate-buffered saline (PBS) and administrated at 10 mg/Kg/day by subcutaneous injection on the back. Control mice received the same volume of PBS. Mice were weighed twice a week. Palpable tumor usually developed in a week. Thirteen mice were used in the control group and 12 were included in the DTG treatment group.

2.11. Metastatic Colony Count

Thirty-three days after inoculation of 4T1 cells, mice were sacrificed. Lungs were collected aseptically, minced, and digested with 5 ml of PBS containing collagenase type IV (ThermoFisher) at 1 mg/ml and elastase (Sigma-Aldrich) at 6 U/ml for 1 hour at 4°C. The suspension was filtered through 70-μM PET-mesh strainer (PluriSelect). Cells were collected by centrifugation at 125 g for 8 minutes, washed with 10-ml of PBS, and resuspend in 10 ml of RPMI1640 with 10% FBS, 6-thioguanine (Cayman Chemical) at 10μg/mL, as well as Antibiotic-Antimycotic (Gibco, with final concentration of penicillin at 100 unit/mL, streptomycin at 100 μg/mL, and amphotericin B at 0.25 μg/mL). Three 10-fold dilutions were made in 100-mm Petri dishes. After incubation at 37°C with 5% CO_2 for 13 days, colonies were stained with crystal violet and counted.

2.12. Statistical Analysis

The Mann-Whitney U test was used for quantitative data. Statistical significance was called at $p<0.05$. Correlation coefficients were tested using the Social Science Statistics Calculator [15]

3. Results

3.1. Dolutegravir (DTG) Inhibits HERV-K and MMTV in cancer cells

Quantitative reverse-transcription PCR (RT-PCR) revealed that dolutegravir inhibited both the *pol* and *env* genes of HERV-K in multiple cell lines including the breast cancer

 doi:10.20944/preprints202202.0223.v1

cell lines MDA-MB-453, SKBR3, BT-20, and T47D, as well as the LNCaP prostate cancer cell line (Figure 1A). The *pol* gene of HERV-K was more significantly inhibited than the *env* gene. DTG also inhibited the expression of the *pol* gene, but not the *env* gene, of MMTV in the murine 4T1 mammary cancer cell line (Figure 1B and C). DTG treatment of BT-20 cells also reduced the genomic copy number of HERV-K, as demonstrated by reduced quantities of both the *pol* and *env* genes (Figure 1D), while the copy number of the *GAPDH* (glyceraldehyde-3-phosphate dehydrogenase) control gene was not affected. Western blot analysis revealed inhibition of the Gag and Env proteins of HERV-K in BT-20 cells (Figure 1E). Using a monoclonal anti-Gag, we were able to detect a 120-kDa (presumably Gag-Pro-Pol) polyprotein, 80-kDa (presumably Gag-Pro) polyprotein, a 44-kDa intermediate product, a 34-kDa product, and a 30-kDa product. The blot in Figure 1E shows the three larger proteins while the blot in Figure 4A reveals more of the smaller Gag products. Using a polyclonal anti-Env, we detected three Env bands of 90 kDa, 68 kDa, and 27 kDa.

Preprints (www.preprints.org) | NOT PEER-REVIEWED | Posted: 18 February 2022 doi:10.20944/preprints202202.0223.v1

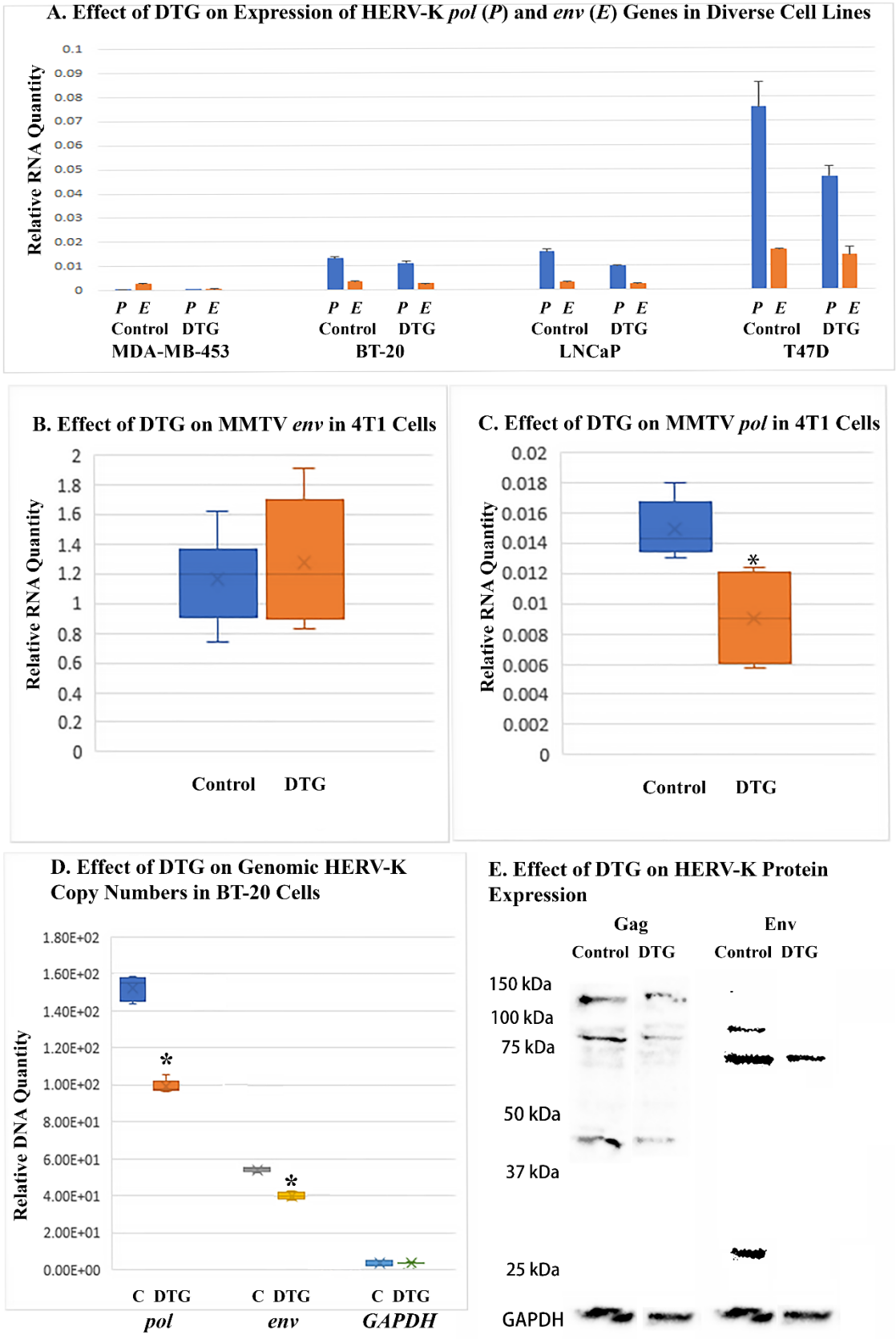

Figure 1. Effect of dolutegravir (DTG) on expression and replication of endogenous retroviruses. (A) shows representative results of quantitative RT-PCR on the expression of HERV-K genes in various cell lines. Cells were treated with DTG at 100 μM (MDA-MB-453 cells), 50 μM (LNCaP cells and BT-20 cells), and 20 μM (T47D cells) for 3-4 days depending on proliferation rates of the cell

 doi:10.20944/preprints202202.0223.v1

lines. Control cells received DMSO solvent. Error bars indicate standard deviations of three technical replicates. (B) and (C) show pooled data of quantitative RT-PCR on the expression of MMTV genes in 4T1 cells using two independent experiments, each with three technical replicates. Cells were treated with DTG at 20 μM or DMSO solvent for 4 days. Asterisk denotes statistically significant difference from solvent-treated control. (D) shows relative abundance of HERV-K proviral DNA in the genome of BT-20 cells as measured with qPCR. Cells were treated with DTG at 50 μM for two days and 75 μM for two more days. DNA quantities were normalized against that of *YWHAZ*. The *GAPDH* gene was used as a negative control. Each treatment included two biological samples, and each sample was quantified in three technical replicates. Asterisks denote statistically significant difference from solvent-treated C cells. (E) shows Western blot analysis of HERV-K Gag and Env proteins upon DTG treatment of BT-20 cells. Cells were treated with DTG at 100 μM or DMSO solvent (control) for 3 days.

3.2. Antiproliferative Effect of DTG Is Correlated with HERV-K Expression

DTG inhibits proliferation of multiple cancer cell lines. The ED50 varied from over 200 μM in MDA-MB-453 cells and SKBR3 cells to under 20 μM in mouse 4T1 cells. In the five human breast and prostate cancer cell lines tested, the antiproliferative effect of DTG is strongly correlated with the expression of HERV-K in control cells. The correlation coefficient between ED50 of DTG and the expression of HERV-K *pol* is 0.99, and that between ED50 and the expression of HERV-K *env* is 0.76, with the former being statistically significant (Figure 2A and B). Figure 2C shows the dosage-dependent antiproliferative effect of DTG on 4T1 cells.

While the correlation between ED50 and HERV-K expression pointed to HERV-K being the mediator of the antiproliferative efficacy of DTG, we found the drug also induced production of reactive oxygen species in the T47D breast cancer cells (Figure 2D). Nelfinavir, a known inducer of ROS, was used as a positive control.

Preprints (www.preprints.org) | NOT PEER-REVIEWED | Posted: 18 February 2022 doi:10.20944/preprints202202.0223.v1

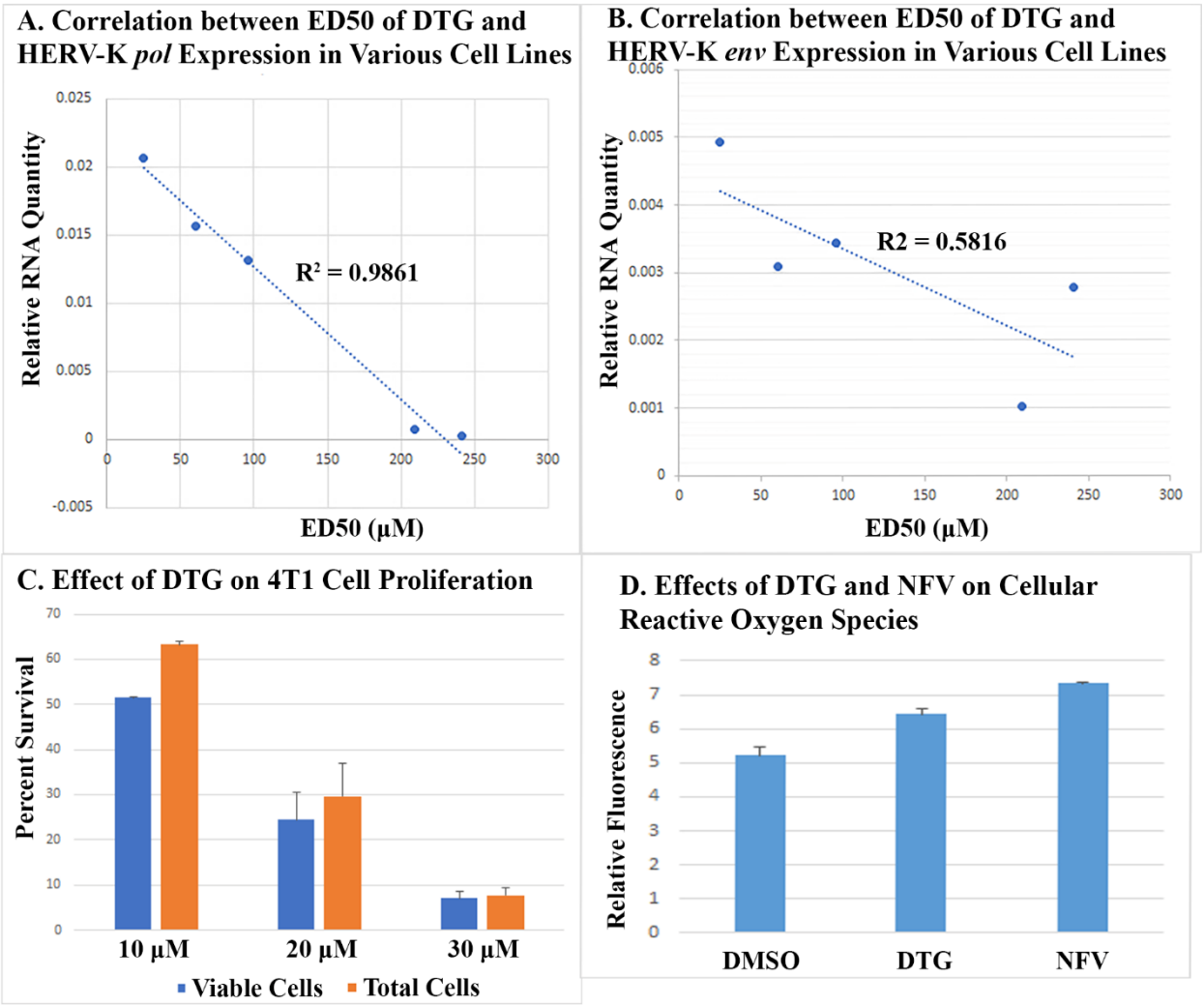

Figure 2. Effect of DTG on cancer cell proliferation. (A) and (B) show correlation between HERV-K expression and ED50 of DTG in five human cancer cell lines (T47D, LNCaP, BT-20, SKBR3, and MDA-B-453 from low to high ED50). Cells were treated with DTG for 3-4 days. ED50 was calculated using the Quest Graph™ ED50 Calculator [16]. Expression of HERV-K genes were measured using quantitative RT-PCR. (C) shows the effect of DTG on the proliferation of mouse 4T1 cells. Cells were treated with DTG for 4 days. Error bars indicate standard deviations of biological duplicates. (D) shows the effect of DTG and nelfinavir (NFV) on the production of reactive oxygen species. Relative fluorescence indicates the amount of cellular reactive oxygen species.

3.3. Overexpressing HERV-K Increased Resistance of BT-20 Cells against DTG

The entire *env* region of HERV-K108, including 98 bases upstream and 112 bases downstream, was cloned into the pLenti-puro vector which expresses target genes under a tet operator. The entire *gag-pro-pol* region of HERV-K107 including 21 bases upstream and 30 bases downstream, was also cloned into the same vector. The constructs were packaged in lentiviral particles, transduced into BT-20 cells, and induced with doxycycline to expression HERV-K genes. Overexpression of the HERV-K genes did not measurably alter the proliferation rate of BT-20 cells (Figure 3B). A cell line stably overexpressing both the *env* and *pol* genes demonstrated significantly enhanced resistance against DTG in the presence of doxycycline (Figure 3B and C). Cell lines transduced with the empty vector, the *env* gene alone, or the *pol* gene alone did not show increased resistance to DTG in the presence of doxycycline (data not shown).

Preprints (www.preprints.org) | NOT PEER-REVIEWED | Posted: 18 February 2022 doi:10.20944/preprints202202.0223.v1

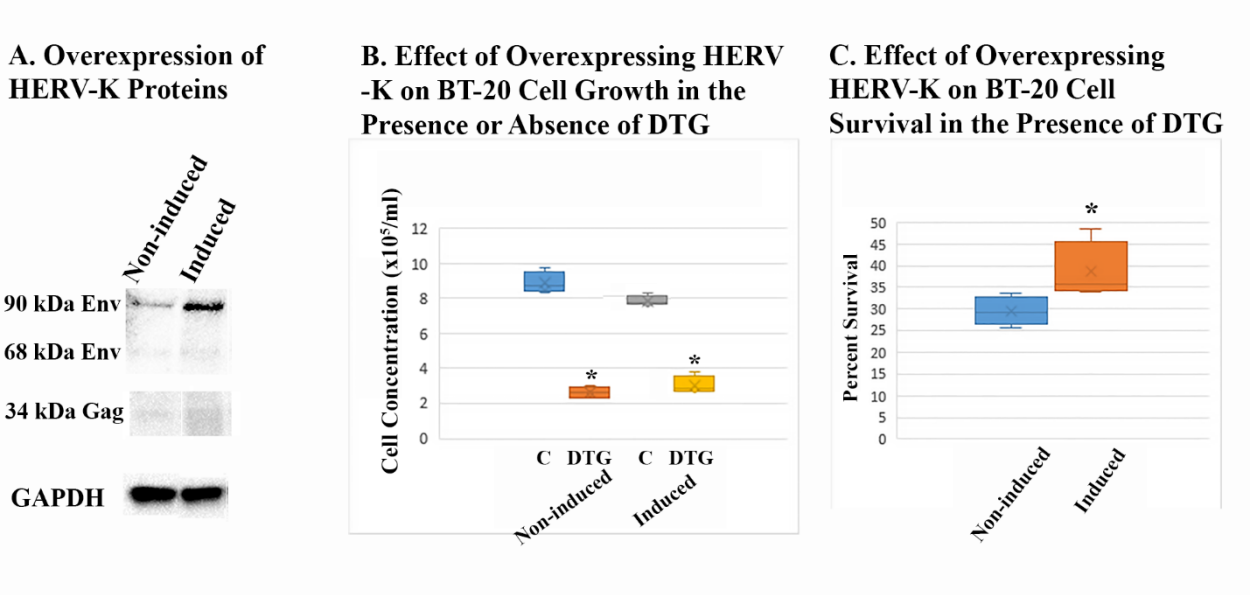

Figure 3. Effect of overexpressing HERV-K on DTG resistance of BT-20 cells. (A) shows Western blot analysis of Env and Gag proteins of HERV-K in overexpressing cells. BT-20 cells transduced with both *env* and *pol* genes of HERV-K under a tet operator were cultured in the absence (non-induced) or presence (induced) of 0.1-µg/mL doxycycline for 5 days. Transduced Env protein was detected using anti-V5 Tag, while Gag was detected using a specific anti-Gag. (B) shows effect of overexpressing both *env* and *pol* on the growth of BT-20 cells in the absence or presence DTG as compared to non-induced cells. Non-induced cells were treated with DTG or DMSO solvent (C denotes solvent control) for 4 days, while induced cells were pretreated with 0.1-µg/mL doxycycline for 24 hours before a 4-day treatment with DTG + doxycycline or solvent + doxycycline. Viable cells were counted in quadruplicate samples. Asterisks denote statistically significant difference from C cells. (C) shows effect of overexpressing HERV-K genes on resistance of BT-20 to DTG. Percent survival was calculated by dividing the number of viable cells in DTG-treated samples with the average number of cells in solvent-treated C samples. Samples were in quadruplets. Asterisk denotes statistically significant difference from non-induced cells.

3.4. Knocking down HERV-K Increased Resistance of BT-20 Cells against DTG

Two HERV-K knockdown lines of BT-20 cells were established, one with shRNA targeting the *pol* region (6175-6203 of the HERV-K108 genome, KD1), and one with shRNA targeting the *pro* region (3327-3355 of the HERV-K108 genome, KD2). Knockdown T47D cells were also established with the same shRNAs. The knockdown cell lines showed decreased proliferation rates and decreased sensitivity to DTG (Figure 4 and Supplementary Figure S1).

Preprints (www.preprints.org) | NOT PEER-REVIEWED | Posted: 18 February 2022 doi:10.20944/preprints202202.0223.v1

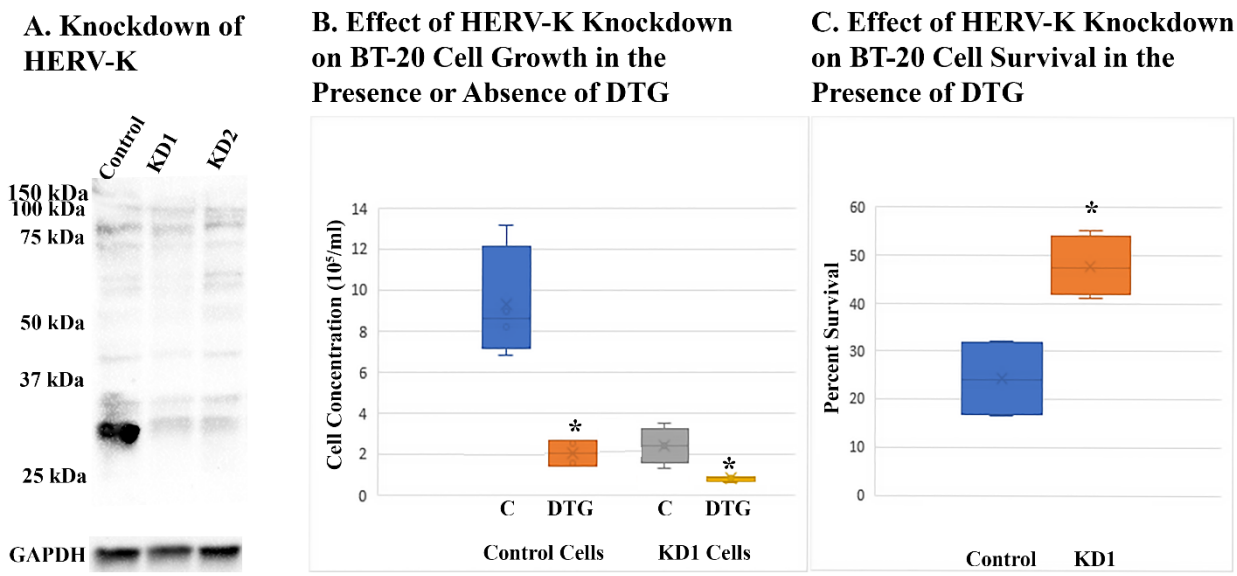

Figure 4. Effect of HERV-K knockdown on DTG resistance of BT-20 cells. (A) shows Western blot analysis of HERV-K expression in two knockdown cell lines, KD1 and KD2, using an anti-Gag. (B) shows effect of HERV-K knockdown on the growth of BT-20 cells in the absence or presence of DTG as compared to control cells which were transduced with the same vector encoding random shRNA. C denotes cells treated with DMSO solvent only. DTG treatment lasted 5 days at 100 μM and 2 additional days at 50 μM. Viable cells were counted in quadruplicate samples. Asterisks denote statistically significant difference from C cells. (C) shows effect of HERV-K knockdown on resistance of BT-20 cells to DTG. Percent survival was calculated by dividing the number of viable cells in DTG-treated samples with the average number of cells in solvent-treated C samples. Samples were in quadruplets. Asterisk denotes statistically significant difference from control cells.

3.5. Effect of DTG on the Cell Cycle of BT-20 Cells Is Similar to HERV-K Knockdown

Cell cycle analyses revealed that DTG kept more cells in G1 and reduced the number of cells in S, G2, and M phases (Figure 5A). HERV-K knockdown resulted in the same pattern of changes (Figure 5B). Cells overexpressing *pol* alone or *pol* + *env* showed decreased number of G1 cells and increased number of S, G2, and M cells, the exact opposite of DTG or HERV-K knockdown, and the effects were more prominent in doubly transduced cells (Figure 5C). BT-20 cells overexpressing the *env* gene alone also showed increased number of G2/M cells, although there was no change in the measured number of G1 cells. Env-driven increase of G2/M cells seemed to be chiefly due to a shortened S phase (Figure 5C).

Preprints (www.preprints.org) | NOT PEER-REVIEWED | Posted: 18 February 2022 doi:10.20944/preprints202202.0223.v1

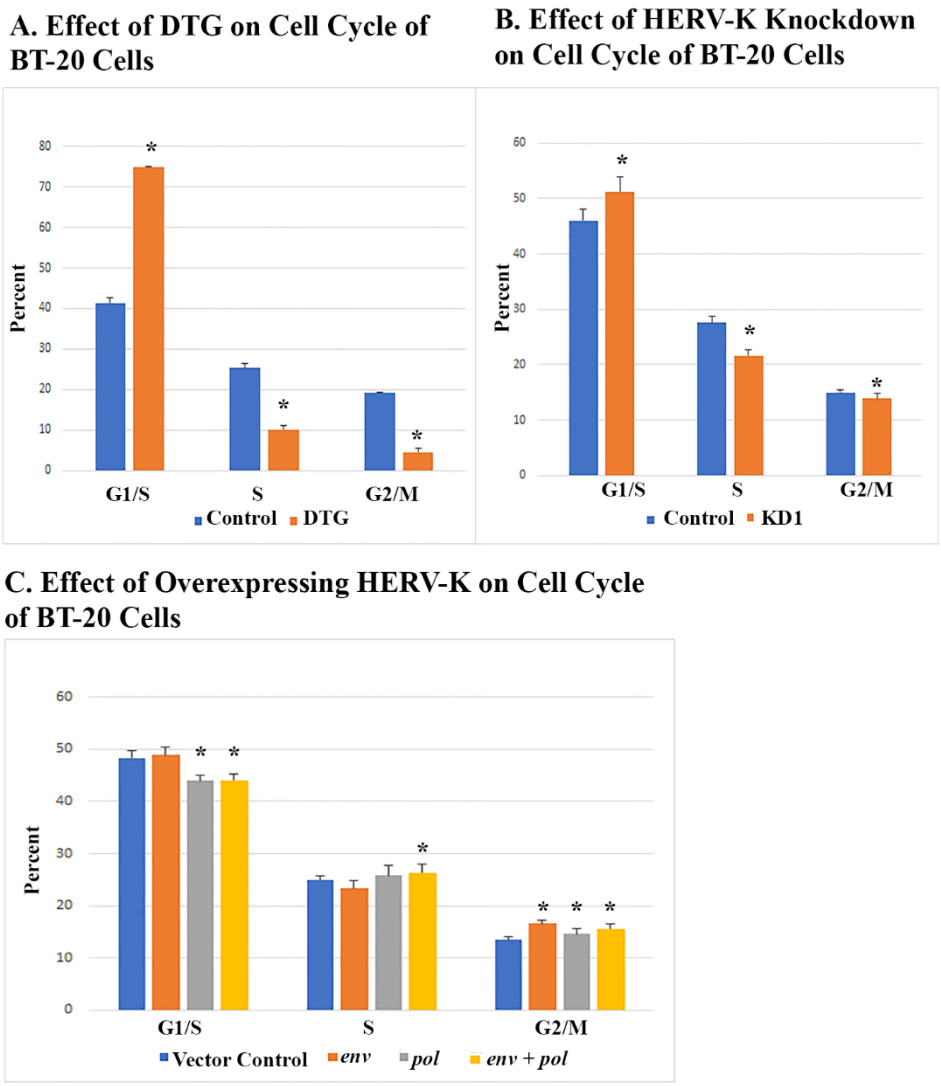

Figure 5. Effect of DTG and HERV-K on BT-20 cell cycle. (A) shows effect of treatment with DTG at 50 μM for 26 hours. Control cells were treated with DMSO solvent. (B) shows effect of HERV-K knockdown. Control cells were transduced with the same vector plasmid expressing random shRNA. (C) shows effect of overexpressing *env* alone, *pol* alone, or both. Control cells were transduced with vector only. All cells were incubated in the presence of 0.1-μg/mL doxycycline for 24 hours. All asterisks denote statistically significant difference from control.

3.6. DTG and HERV-K Knockdown Both Inhibits Cell Motility and Invasiveness

DTG and HERV-K knockdown both increased expression of E-Cadherin in BT-20 cells (Figure 6A). Since loss of E-Cadherin expression has been associated with epithelial-mesenchymal transition (EMT) and metastasis, we measured the motility of BT-20 cells in the presence of DTG using a wound-healing assay. As expected, DTG treatment reduced motility of BT-20 cells, so did HERV-K knockdown (Figure 6B, D, and E). A transwell assay revealed reduced invasiveness of BT-20 cells through the basement membrane extract in the presence of DTG, an effect similar to that of HERV-K knockdown (Figure 6C, F, and G).

Preprints (www.preprints.org) | NOT PEER-REVIEWED | Posted: 18 February 2022 doi:10.20944/preprints202202.0223.v1

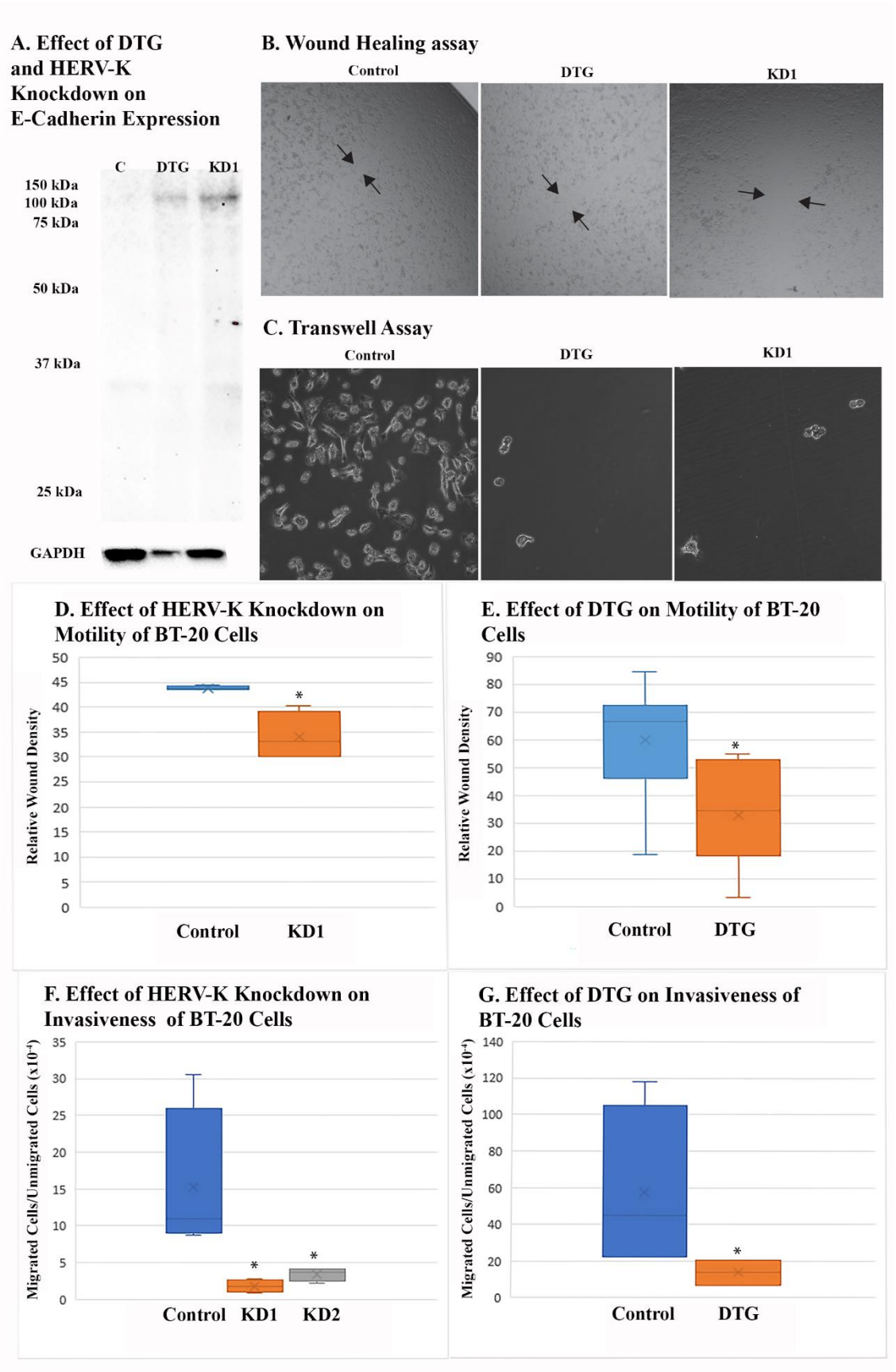

Figure 6. Effect of DTG on motility and invasiveness of BT-20 cells as compared with HERV-K knockdown. (A) shows Western blot analysis of E-Cadherin expression in DTG-treated or knock-down cells. Cells transduced with random shRNA were treated with solvent only (C) or DTG at 50 μM for 5 days. KD1 cells were treated with DMSO solvent. A monoclonal anti-E-Cadherin was used.

Preprints (www.preprints.org) | NOT PEER-REVIEWED | Posted: 18 February 2022 doi:10.20944/preprints202202.0223.v1

(B) Wound healing assay. Control cells were transduced with vector plasmid encoding random shRNA. DTG cells were pretreated with 50-μM DTG for 48 hours and the treatment continued during wound healing. Images represent wounded area after 22 hours. (C) Transwell assay. DTG cells were pretreated with 50-μM DTG or solvent for 24 hours and the treatment continued during the assay. Images were taken after 65 hours. (D) and (E) Results of wound healing assay in terms of relative wound density. Control cells in D were transduced with plasmid encoding random shRNA while control cells in E were treated with DMSO solvent. (F) and (G) Results of transwell assay in terms of the ratio of migrated cells to unmigrated cells. All asterisks denote statistically significant difference from control.

3.7. DTG Enhanced HERV-K env Expression and Metastasis of 4T1 Cells in Vivo

In BALB/c mice inoculated with 4T1 cells orthotopically, treatment with DTG did not affect the size of mammary tumors (Figure 7A). Surprisingly, DTG increased the number of metastatic cells in the lungs (Figure 7B), but this was associated with increased expression of MMTV *env* in tumor tissues of DTG-treated mice. Levels of *env* gene expression in tumor tissues were positively correlated with both tumor mass and metastatic colony count.

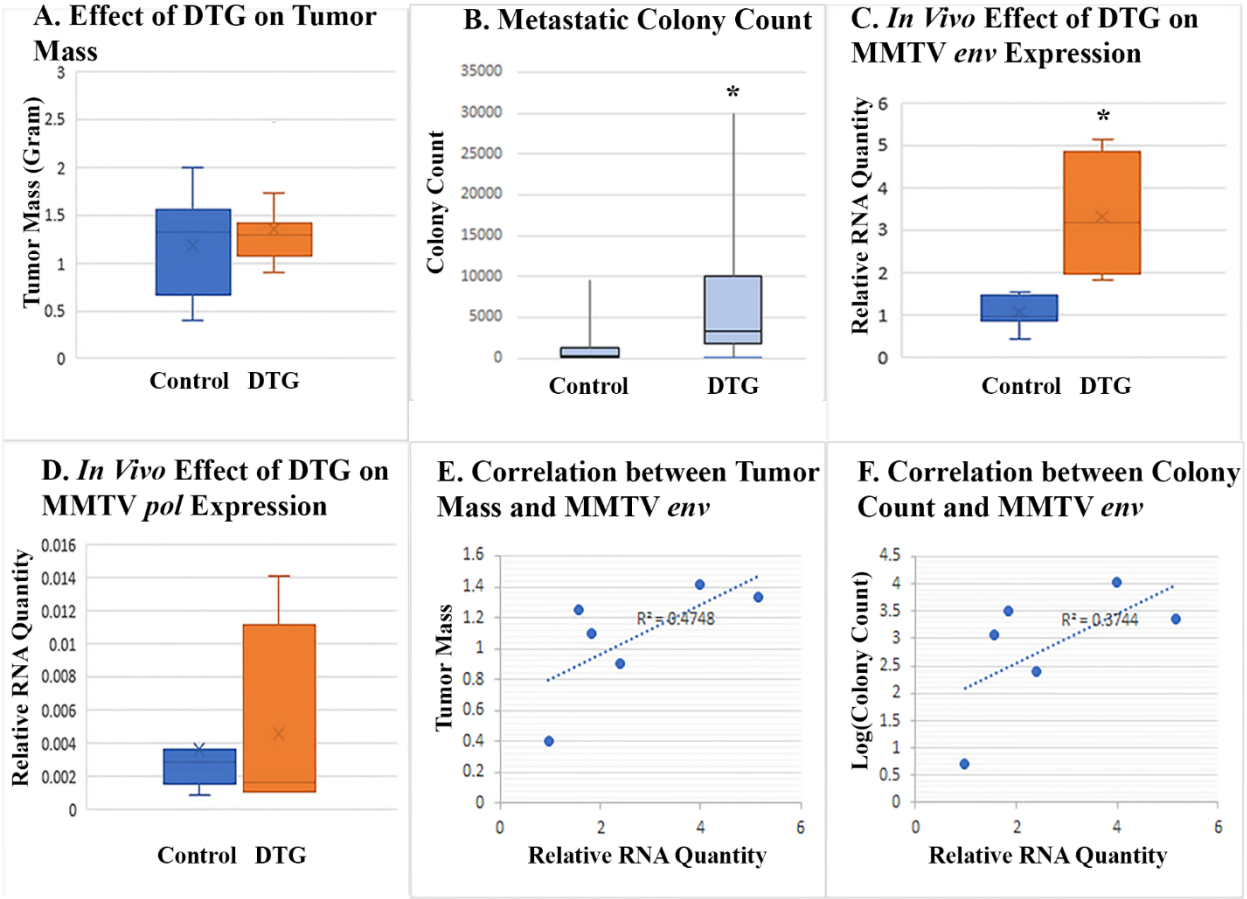

Figure 7. *In vivo* effect of DTG on tumor growth and MMTV expression. (A) shows average tumor mass in DTG-treated mice versus solvent-treated mice. (B) shows number of metastatic cells in lungs of DTG-treated mice versus solvent-treated mice. Metastatic cells were represented as thioguanine-resistant colonies grown from digested lungs. (C) and (D) show effect of DTG on MMTV expression in tumor tissues as measured with quantitative RT-PCR. (E) and (F) show correlation between MMTV *env* expression in tumor tissue and tumor mass or metastatic colony count. Asterisks denote statistically significant difference from control.

4. Discussion

 doi:10.20944/preprints202202.0223.v1

Although there have been endeavors to use antiretroviral agents to inhibit cancer cell proliferation *in vitro* and cancer growth *in vivo* [**Error! Bookmark not defined.**-**Error! Bookmark not defined.**, 8–11], this study is the first published attempt to prove that an antiretroviral agent exerts its antineoplastic effect through inhibition of an ERV. DTG has been reported to increase intracellular calcium level and induce oxidative stress in erythrocytes [17]. Our finding of increased ROS in T47D breast cancer cells suggests this mechanism as well. A DTG derivative is known to inhibit proliferation of non-small cell lung cancer cells through the calcium signaling pathway [18]. In agreement with such findings, our data indicate that ERV inhibition is not the only antineoplastic mechanism of DTG, since neither overexpressing HERV-K genes nor knockdown of HERV-K renders BT-20 cells completely resistant to DTG.

Because HERVs are mostly degenerate and not actively transposing in the human genome, the inhibitory effect of INSTIs on HERV-K came as a surprise. Our finding of the effect of dolutegravir on genomic copy number of HERV-K indicates dynamic changes of HERV-K on the DNA level in BT-20 cells. Since the copy number of HERV-W is known to increase in peripheral blood mononuclear cells of patients with multiple sclerosis [19], it is conceivable for the more intact HERV-K to be actively transposing in malignant cancers.

The integrase plays other roles in retroviral replication beside integration of proviral DNA into host chromosomes. Cleavage of episomal 2-LTR circles and integration of episomal proviral DNA into linear concatemers are also functions of the integrase [20, 21,22]. These episomal forms of viral DNA are transcribed to various degrees [23]. In addition, the integrase also plays roles in reverse transcription, recruitment of host proteins into the viral particle, as well as viral maturation [24]. Even without new insertion events, INSTIs can affect many aspects of ERV activities in host cells.

Surprisingly, the inhibitory effect of DTG on MMTV *pol* observed *in vitro* became insignificant *in vivo* and the drug significantly enhanced *env* expression *in vivo*, accompanied by enhanced metastasis. These results support previous findings of the HERV-K Env in driving cancer cell proliferation and EMT [**Error! Bookmark not defined.**,**Error! Bookmark not defined.**]. The *in vivo* ERV-stimulating effect of DTG may have to do with oxidative stress, which would inhibit DNA methylation and histone deacetylation [25]. The levels of ROS tend to be high in the tumor microenvironment [26], and DTG exacerbates this phenomenon. Alternatively, DTG may have a negative effect on anti-tumor immunity since ERVs are known to contribute to normal immune responses [27]. MMTV transcripts and antigens are known targets of anti-tumor immunity [28]. Such results highlight the dilemma between inhibiting tumorigenic ERVs with antiretroviral drugs and targeting ERVs in cancer immunotherapy [29]. Combined antiretroviral agents and ERV-targeting immunotherapy may show some additive effect.

Since there are some fundamental differences between human and mouse ERVs and between human and mouse immune systems, using xenograft models to study the effect of DTG on human breast cancers may yield different results from what we observed in the mouse tumor model.

Author Contributions: Conceptualization, Yingguang Liu; Investigation, Jiayi Li, John Lin, John Lin, Mason Farris, Lauren Robbins, Leo Andrada, Bryce Grohol, Serratt Nong and Yingguang Liu; Methodology, Jiayi Li and Yingguang Liu; Supervision, Yingguang Liu; Validation, Jiayi Li and Yingguang Liu; Visualization, Yingguang Liu; Writing – original draft, Yingguang Liu; Writing – review & editing, Jiayi Li, John Lin, John Lin, Mason Farris, Lauren Robbins, Leo Andrada, Bryce Grohol and Yingguang Liu.

Funding: This research received no external funding.

Acknowledgements: We thank Jeffrey Houghton for technical support. Drs. Anthony Bauer, Joseph Gigliotti, James Swanson, and Michael Price helped with animal management, provided technical assistance, and kindly contributed ideas and reagents. We thank Dr. Joseph Gigliotti for critical reading of the manuscript.

Conflicts of Interest: The authors declare no conflict of interest.

Preprints (www.preprints.org) | NOT PEER-REVIEWED | Posted: 18 February 2022 doi:10.20944/preprints202202.0223.v1

Appendix: Supplementary data

Table S1. Primers for quantitative PCR.

Gene	Forward	Reverse	Reference
HERV-K *pol*	CACTCAAGAGGCAGGAGTTAAT	GGCCTGTCCTTGGGAATTAT	
HERV-K *env*	ATTGGCAACACCGTATTCTGCT	CAGTCAAAATATGGACGGATGGC	
MMTV *env*	TTAGTTAAGGAGATGCAAACTGC	CACATCTTGTCCCAACTCTAAAAC	
MMTV *pol*	GACCAGCCTGTATGGCTTAAT	GAGGAGCGAGCAGGTGAACT	
Mouse Pgk1	GCAGATTGTTTGGAATGGTC	TGCTCACATGGCTGACTTTA	
GAPDH	AACTTTGGCATTGTGGAAGG	GCAGGGATGATGTTCTGG	
YWHAZ	ACTTTTGGTACATTGTGGCTTCAA	CCGCCAGGACAAACCAGTAT	14

Table S2. Primers for cloning.

Gene	Forward	Reverse	Reference sequence
HERV-K *pol*	GTCGACTAGTGGATCTCGGAAGAAGCTAGGGTGATAATGG	ATAGGCTTACCTTCGTCCTGGTGAAACACAAGCAAAACC	1091-6411 of AF164613.1
HERV-K *env*	GTCGACTAGTGGATCAGGGAAGGTGATAACGTGGGG	ATAGGCTTACCTTCGCATGTTTCAGAGAGCACGGGG	30253-32563 of AC072054.10
MMTV *pol*	GAGATCGTCGACTAGGCAGTCTCGCCTACAGAGAAG	GATGACCGGTACGCGAGAGGTTTGGGGAGTTTGTGA	
MMTV *env*	CAGTGTGGTGGAATTGGACGAGGCTATGCTTGTGTT	GCCCTCTAGACTCGACGTCCTTGGTGGGAAACAAC	

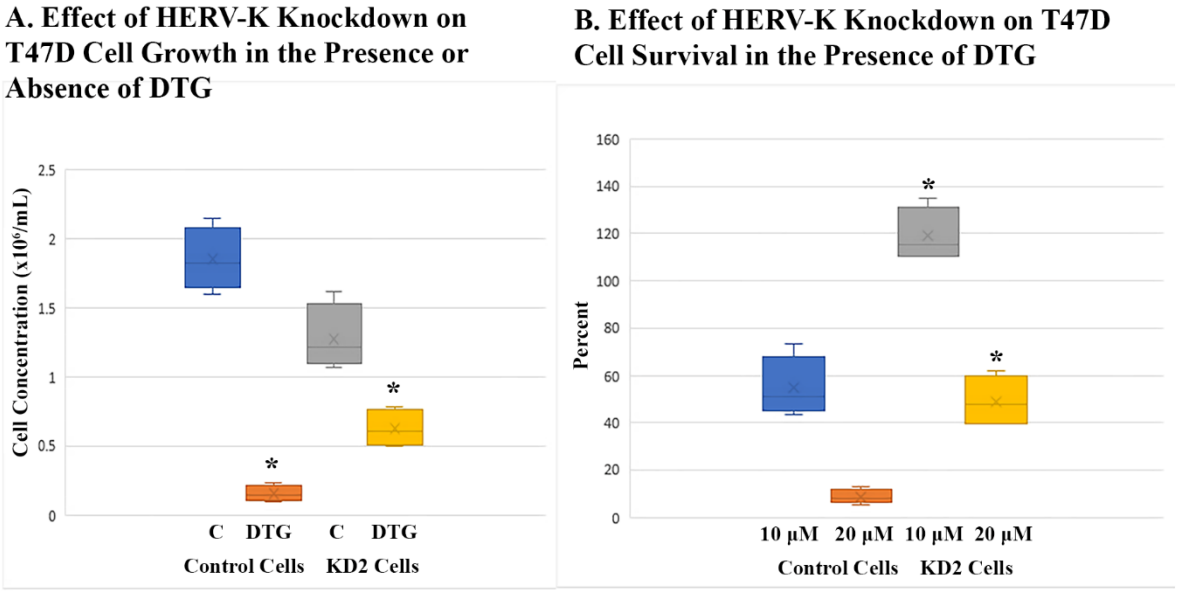

Figure S1. Effect of HERV-K knockdown on DTG resistance of T47D cells. (A) shows effect of HERV-K knockdown on the growth of T47D cells in the absence or presence of DTG as compared to control cells which were transduced with the same vector encoding random shRNA. C denotes cells treated with DMSO solvent. DTG treatment lasted 5 days at 20 μM. Total cells were counted in quadruplicate samples. Asterisks denote statistically significant difference from C cells. (B) shows effect of HERV-K knockdown on resistance of T47D cells to DTG at two drug concentrations. Percent survival was calculated by dividing the number of total cells in DTG-treated samples with the average number of cells in solvent-treated C samples. Samples were in quadruplets. Asterisks denote statistically significant difference from control cells treated with DTG at the same concentration.

References

1. Grow EJ, Flynn RA, Chavez SL, et al. Intrinsic retroviral reactivation in human preimplantation embryos and pluripotent cells. *Nature* 2015;522(7555):221-225. doi:10.1038/nature14308.

2. Gonzalez-Cao M, Iduma P, Karachaliou N, Santarpia M, Blanco J, Rosell R. Human endogenous retroviruses and cancer. *Cancer Biol Med* 2016;13(4):483-488. doi:10.20892/j.issn.2095-3941.2016.0080.

3. Zhou F, Li M, Wei Y, et al. Activation of HERV-K Env protein is essential for tumorigenesis and metastasis of breast cancer cells. *Oncotarget* 2016;7(51):84093-84117. doi:10.18632/oncotarget.11455.

4. Lemaître C, Tsang J, Bireau C, Heidmann T, Dewannieux M. A human endogenous retrovirus-derived gene that can contribute to oncogenesis by activating the ERK pathway and inducing migration and invasion. *PLoS Pathog* 2017;13(6):e1006451. Published 2017 Jun 26. doi:10.1371/journal.ppat.1006451.

5. Nguyen TD, Davis J, Eugenio RA, Liu Y. Female Sex Hormones Activate Human Endogenous Retrovirus Type K Through the OCT4 Transcription Factor in T47D Breast Cancer Cells. *AIDS Res Hum Retroviruses* 2019;35(3):348-356. doi:10.1089/AID.2018.0173.

6. Sciamanna I, Landriscina M, Pittoggi C, et al. Inhibition of endogenous reverse transcriptase antagonizes human tumor growth. *Oncogene* 2005;24(24):3923-3931. doi:10.1038/sj.onc.1208562.

7. Landriscina M, Fabiano A, Altamura S, et al. Reverse transcriptase inhibitors down-regulate cell proliferation in vitro and in vivo and restore thyrotropin signaling and iodine uptake in human thyroid anaplastic carcinoma. *J Clin Endocrinol Metab* 2005;90(10):5663-5671. doi:10.1210/jc.2005-0367.

8. Tyagi R, Li W, Parades D, Bianchet MA, Nath A. Inhibition of human endogenous retrovirus-K by antiretroviral drugs. *Retrovirology* 2017;14(1):21. doi:10.1186/s12977-017-0347-4.

9. Kawabata S, Connis N, Gills JJ, Hann CL, Dennis PA. Nelfinavir Inhibits the Growth of Small-cell Lung Cancer Cells and Patient-derived Xenograft Tumors. *Anticancer Res* 2021;41(1):91-99. doi:10.21873/anticanres.14754.

10. Shim JS, Rao R, Beebe K, et al. Selective inhibition of HER2-positive breast cancer cells by the HIV protease inhibitor nelfinavir. *J Natl Cancer Inst* 2012;104(20):1576-1590. doi:10.1093/jnci/djs396.

11. Patnala R, Lee SH, Dahlstrom JE, et al. Inhibition of LINE-1 retrotransposon-encoded reverse transcriptase modulates the expression of cell differentiation genes in breast cancer cells. *Breast Cancer Res Treat* 2014;143(2):239-253. doi:10.1007/s10549-013-2812-7.

12. Soprano M, Sorriento D, Rusciano MR, et al. Oxidative Stress Mediates the Antiproliferative Effects of Nelfinavir in Breast Cancer Cells. *PLoS One* 2016;11(6):e0155970. doi:10.1371/journal.pone.0155970.

13. Toegel S, Huang W, Piana C, et al. Selection of reliable reference genes for qPCR studies on chondroprotective action. *BMC Mol Biol* 2007;8:13. Published 2007 Feb 26. doi:10.1186/1471-2199-8-13.

14. Grada A, Otero-Vinas M, Prieto-Castrillo F, Obagi Z, Falanga V. Research Techniques Made Simple: Analysis of Collective Cell Migration Using the Wound Healing Assay. *J Invest Dermatol* 2017;137(2):e11-e16. doi:10.1016/j.jid.2016.11.020.

15. P Value from Pearson R Calculator. Available online: https://www.socscistatistics.com/pvalues/pearsondistribution.aspx (accessed on January 31, 2022).

16. Quest Graph™ ED50 Calculator. Available online: https://www.aatbio.com/tools/ed50-calculator (accessed on February 1, 2022).

17. Al Mamun Bhuyan A, Signoretto E, Bissinger R, Lang F. Enhanced Eryptosis Following Exposure to Dolutegravir. *Cell Physiol Biochem* 2016;39(2):639-650. doi:10.1159/000445655.

18. Wang WJ, Mao LF, Lai HL, et al. Dolutegravir derivative inhibits proliferation and induces apoptosis of non-small cell lung cancer cells via calcium signaling pathway. *Pharmacol Res* 2020;161:105129. doi:10.1016/j.phrs.2020.105129.

19. Garcia-Montojo M, Dominguez-Mozo M, Arias-Leal A, et al. The DNA copy number of human endogenous retrovirus-W (MSRV-type) is increased in multiple sclerosis patients and is influenced by gender and disease severity. *PLoS One* 2013;8(1):e53623. doi:10.1371/journal.pone.0053623.

20. Delelis O, Petit C, Leh H, Mbemba G, Mouscadet JF, Sonigo P. A novel function for spumaretrovirus integrase: an early requirement for integrase-mediated cleavage of 2 LTR circles. *Retrovirology* 2005;2:31. doi:10.1186/1742-4690-2-31.

21. Richetta C, Thierry S, Thierry E, et al. Two-long terminal repeat (LTR) DNA circles are a substrate for HIV-1 integrase. *J Biol Chem* 2019;294(20):8286-8295. doi:10.1074/jbc.RA118.006755.

22. Brooun A, Richman DD, Kornbluth RS. HIV-1 preintegration complexes preferentially integrate into longer target DNA molecules in solution as detected by a sensitive, polymerase chain reaction-based integration assay. *J Biol Chem* 2001;276(50):46946-46952. doi:10.1074/jbc.M108000200.

23. Cara A, Cereseto A, Lori F, Reitz MS Jr. HIV-1 protein expression from synthetic circles of DNA mimicking the extrachromosomal forms of viral DNA. *J Biol Chem* 1996;271(10):5393-5397. doi:10.1074/jbc.271.10.5393.

24. Grandgenett DP, Pandey KK, Bera S, Aihara H. Multifunctional facets of retrovirus integrase. *World J Biol Chem* 2015;6(3):83-94. doi:10.4331/wjbc.v6.i3.83.

25. Morris G, Maes M, Murdjeva M, Puri BK. Do Human Endogenous Retroviruses Contribute to Multiple Sclerosis, and if So, How?. *Mol Neurobiol* 2019;56(4):2590-2605. doi:10.1007/s12035-018-1255-x.

26. Lin HJ, Liu Y, Lofland D, Lin J. Breast Cancer Tumor Microenvironment and Molecular Aberrations Hijack Tumoricidal Immunity. *Cancers (Basel)* 2022;14(2):285. Published 2022 Jan 7. doi:10.3390/cancers14020285.

27. Greenig M. HERVs, immunity, and autoimmunity: understanding the connection. *PeerJ* 2019;7:e6711. Published 2019 Apr 5. doi:10.7717/peerj.6711.

28. Lopez DM. Humoral and cellular immune responses to mouse mammary tumor virus (MMTV) in experimental animal models (review). *Anticancer Res* 1984;4(4-5):305-312.

29. Cherkasova E, Weisman Q, Childs RW. Endogenous retroviruses as targets for antitumor immunity in renal cell cancer and other tumors. *Front Oncol* 2013;3:243. Published 2013 Sep 17. doi:10.3389/fonc.2013.00243.